Published in final edited form as:
Int J Cancer. 2011 February 15; 128(4): 920–926. doi:10.1002/ijc.25409.

PET imaging of tumor angiogenesis in mice with VEGF-A targeted ^{86}Y-CHX-A″-DTPA-bevacizumab

Tapan K. Nayak[*], **Kayhan Garmestani**, **Kwamena E. Baidoo**, **Diane E. Milenic**, and **Martin W. Brechbiel**
Radioimmune & Inorganic Chemistry Section, Radiation Oncology Branch, National Cancer Institute, National Institute of Health, Bethesda, MD-20892, USA

Abstract

Bevacizumab is a humanized monoclonal antibody that binds to tumor-secreted VEGF-A and inhibits tumor angiogenesis. In 2004, the antibody was approved by the United States FDA for the treatment of metastatic colorectal carcinoma in combination with chemotherapy. This report describes the preclinical evaluation of a radioimmunoconjugate, ^{86}Y-CHX-A″-DTPA-bevacizumab, for potential use in PET imaging of VEGF-A tumor angiogenesis and as a surrogate marker for ^{90}Y based radioimmunotherapy. Bevacizumab was conjugated to CHX-A″-DTPA and radiolabeled with ^{86}Y. *In vivo* biodistribution and PET imaging studies were performed on mice bearing VEGF-A secreting human colorectal (LS-174T), human ovarian (SKOV-3) and VEGF-A negative human mesothelioma (MSTO-211H) xenografts. Biodistribution and PET imaging studies demonstrated high specific tumor uptake of the radioimmunoconjugate. In mice bearing VEGF-A secreting LS-174T, SKOV-3 and VEGF-A negative MSTO-211H tumors, the tumor uptake at 3 d post-injection (p.i) was 13.6 ± 1.5, 17.4 ± 1.7 and 6.8 ± 0.7 % ID/g, respectively. The corresponding tumor uptake in mice co-injected with 0.05 mg cold bevacizumab were 5.8 ± 1.3, 8.9 ± 1.9 and 7.4 ± 1.0 % ID/g, respectively at the same time point, demonstrating specific blockage of the target in VEGF-A secreting tumors. The LS-174T and SKOV3 tumors were clearly visualized by PET imaging after injecting 1.8–2.0 MBq ^{86}Y-CHX-A″-DTPA-bevacizumab. Organ uptake quantified by PET closely correlated (r^2=0.87, p=0.64, n=18) to values determined by biodistribution studies. This preclinical study demonstrates the potential of the radioimmunoconjugate, ^{86}Y-CHX-A″-DTPA-bevacizumab, for non-invasive assessment of the VEGF-A tumor angiogenesis status and as a surrogate marker for ^{90}Y-CHX-A″-DTPA-bevacizumab radioimmunotherapy.

Keywords

PET imaging; VEGF-A; Angiogenesis; Bevacizumab; ^{86}Y

Introduction

Abnormal angiogenesis, one of the hallmarks of cancer, is characterized by an increase in the number of proliferating endothelial cells and altered morphology of the vasculature resulting in increased tumor cell migration and proliferation [1, 2]. The vascular endothelial growth factor (VEGF) is a proangiogenic factor that is secreted by stromal or cancer cells [2, 3]. The tumor secreted VEGF promotes tumor survival, migration and invasion and is

[*]First author (Post-doctoral fellow) and corresponding author: Tapan K. Nayak, Building 10, Room 1B40, NCI-Bethesda, Bethesda, MD 20892. Fax: 301-402-1923. Phone: 301-443-1038, tapann@gmail.com.

Authors declare no conflict of interests.

therefore an important target for cancer therapy [2, 3]. The VEGF family is comprised of five VEGF glycoproteins (VEGF-A, VEGF-B, VEGF-C, VEGF-D and VEGF-E). VEGF-A is the best characterized of these glycoproteins and encodes three main isoforms: $VEGF_{121}$, $VEGF_{165}$ and $VEGF_{189}$ [3]. VEGF mediates its angiogenic effects via several tyrosine kinase receptors. Of these, VEGFR-2 mediates the majority of VEGF-A signaling in the tumor microenvironment including microvascular permeability and endothelial cell proliferation [3, 4]. Several agents, including antibodies and soluble receptor constructs, have been developed to target the VEGF system. Bevacizumab, a recombinant humanized monoclonal antibody (mAb) to VEGF-A, is approved by the United States FDA and the European Medicines Agency for the treatment of metastatic colorectal cancer, non-small-cell lung cancer, breast cancer and glioblastoma multiforme in combination with chemotherapy [5, 6]. One of the greatest challenges in bevacizumab therapy is the lack of predictive biomarkers and tools that can predict the efficacy of anti-VEGF therapy [6]. Molecular imaging techniques such as dynamic-contrast enhanced magnetic resonance imaging (DCE-MRI) and nuclear imaging modalities have been investigated to assess response to bevacizumab therapy [7–9]. With respect to nuclear imaging, bevacizumab was radiolabeled with ^{89}Zr and ^{111}In for PET and SPECT imaging, respectively, to screen patients that may respond to therapy, [10–12].

Previously, reports from this laboratory have described the use of ^{86}Y ($t_{1/2}$ = 14.7 h) as a positron-emitting radionuclide for radioimmunoimaging of HER1 and HER2-expressing carcinoma [13–15]. In this study, the well-established bifunctional chelate, CHX-A″-DTPA was conjugated to bevacizumab and radiolabeled with ^{86}Y as an alternative bevacizumab PET imaging agent. ^{86}Y was selected due to its well-established chelation chemistry, and reasonable availability [13, 16]. In addition to these attractive features, ^{86}Y can also serve as a surrogate PET marker for ^{90}Y-CHX-A″-DTPA-bevacizumab radioimmunotherapy (RIT) of solid tumors [17]. The primary use of such an agent would be for the selection of patients for bevacizumab targeted therapy, monitoring of patients undergoing such therapy and to provide information for dosimetric calculations for patients receiving ^{90}Y-CHX-A″-DTPA-bevacizumab.

Methods and Materials

Preparation of ^{86}Y-CHX-A″-DTPA-bevacizumab

^{86}Y was produced by the $^{86}Sr(p, n)^{86}Y$ reaction as previously described, with minor modifications in post-irradiation processing of the $SrCO_3$ target [13]. The bifunctional chelate, CHX-A″-DTPA, was conjugated to bevacizumab as previously described with minor modification and the chelate to protein ratios determined using the arsenazo assay [18]. For radiolabeling, a freshly prepared solution of ascorbic acid (50 μL, 220 μg/μL) was first added to the ^{86}Y solution (140–170 MBq in 0.1 M nitric acid, 500 μL) to prevent radiolysis. The acidic solution was neutralized to pH 6 by the addition of a solution of ammonium acetate buffer (50 μL, 5 M, pH 7.0). CHX-A″-DTPA-bevacizumab (50 μg in 0.15 M ammonium acetate solution) was added to the mixture, vortexed briefly, and then incubated at room temperature for 30 min. The reaction was quenched by the addition of EDTA solution (4 μL, 0.1 M). The radiolabeled product was purified using a PD-10 desalting column (GE Healthcare, Piscataway, NJ, USA). Size exclusion HPLC chromatography using a TSK-3000 column (Toso-Haas, Montgomeryville, PA, USA) was performed to ascertain the purity of the radioimmunoconjugate (RIC).

Radioimmunoassay (RIA)

Integrity of the ^{86}Y-CHX-A″-DTPA-bevacizumab was determined by an RIA based immunoreactivity assay using recombinant human VEGF165 (R&D systems, Minneapolis, MN, USA) as the target antigen. The recombinant human VEGF165 was diluted in PBS to a

concentration of 50 ng/100 μL, added to the wells (100 μL) of Nunc Immuno BreakApart plates and incubated overnight at 4°C. The wells were aspirated, 150 μL of 1% BSA/PBS was added to the wells and allowed to incubate at room temperature for 1 h. The 1% BSA/PBS was removed, serial dilutions of ^{86}Y-CHX-A″-DTPA-bevacizumab were added to the wells, and 1 μM of excess bevacizumab was added to a different set of wells to determine non-specific binding. Following a 4 h incubation at room temperature, the reaction mixture was washed twice with 200 μL 1% BSA/PBS and the antigen-antibody complex collected by adding 100 μL of 0.2 M NaOH to each well. After 15 min at room temperature, the NaOH solution was absorbed onto cotton filters and counted on a gamma counter (WizardOne, Shelton, CT, USA). The percentage of binding was calculated as the fraction of radioactivity stacked to antigen-coated wells divided by the total amount of radioactivity added.

Cell culture

VEGF-A secreting human colorectal (LS-174T) [11] and human ovarian (SKOV3) carcinoma cells [10] and VEGF-A negative human biphasic mesothelioma (MSTO-211H) cells [19] were purchased from American Type Culture Collection (Rockville, MD, USA). All cell lines were grown as a monolayer at 37° C, in a humidified atmosphere of 5% CO_2 and 95% air. LS-174T cells were cultured in Dulbecco's minimal essential medium containing 10 mM glutamine solution. SKOV3 cells were cultured in McCoy's media, while the MSTO-211H cells were cultured in RPMI-1640 media containing 2 mM L-glutamine, 10 mM HEPES, 1 mM sodium pyruvate, 4500 mg/L glucose, and 1500 mg/L sodium bicarbonate. All media were additionally supplemented with 10% FetalPlex (Gemini Bio-Products, Inc, Woodland, CA, USA). Media and supplements were obtained from Invitrogen (Carlsbad, CA, USA) and Lonza (Walkersville, MD, USA).

Animal and tumor models

Female athymic *nu/nu* mice (Charles River Laboratory, Frederick, MD, USA) were injected subcutaneously with a single-cell suspension (200 μL medium containing 20% matrigel) of 2 million VEGF-A positive LS-174T cells. In another set of experiments, mice were injected with 2 million VEGF-A positive SKOV3 cells on the left leg. Two weeks later, the mice bearing SKOV-3 tumors were injected s.c. with 2 million VEGF-A negative MSTO-211H cells on the opposite leg.

In vivo evaluations

Biodistribution and pharmacokinetics studies—Female athymic mice bearing VEGF-A secreting human colorectal (LS-174T) or ovarian (SKOV3) and VEGF-A negative biphasic mesothelioma (MSTO-211H) xenografts were injected intravenously (i.v) via the tail vein with 0.5 MBq/3 μg of ^{86}Y-CHX-A″-DTPA-bevacizumab. To determine VEGF-A-specificity, bevacizumab (0.05 mg) was co-injected with the RIC. This sub-saturation dose was selected to avoid physiological and vascular effects of high-dose bevacizumab. At the desired time points, the animals were sacrificed by CO_2 inhalation and the blood, tumor and select organs were harvested to determine the biodistribution characteristics of the RIC. The samples were wet-weighed and the radioactivity measured. The percent injected dose per gram (% ID/g) of tissue was calculated by comparison with standards representing 10% of the injected dose per animal. Non-compartmental pharmacokinetics was performed to determine AUC, AUMC and the MRT using trapezoidal integration analysis.

PET imaging studies—Female athymic mice bearing LS-174T, SKOV3 and MSTO-211H xenografts were injected i.v with 1.8–2.0 MBq/3 μg of ^{86}Y-CHX-A″-DTPA-bevacizumab. To determine VEGF-A-specificity and localization, excess bevacizumab (0.05

mg) was co-injected with the RIC. Small animal PET studies were performed using the ATLAS (Advanced Technology Laboratory Animal Scanner) at the National Institute of Health, Bethesda, MD, USA. Whole body imaging studies (6 bed positions, total acquisition time of 1 h per mouse) were carried out on anesthetized mice (1.5–1.7% isoflurane) on a temperature-controlled bed as previously described [15]. The mice were euthanized and *ex vivo* biodistribution studies were performed to determine the correlation between the *in vivo* PET-assessed % ID/cm^3 and the *ex vivo* biodistribution determined % ID/g. The animal studies were performed in accordance with the NIH guidelines for the humane use of animals and all procedures were reviewed and approved by the Institutional Animal Care and Use Committee.

Statistical Analysis

All numerical data were expressed as the mean of the values ± the standard error of mean (SEM). Graphpad Prism version 5 (San Diego, CA, USA) was used for statistical analysis. A p value less than 0.05 was considered statistically significant.

Results

Radiochemistry and *In vitro* evaluations

The ^{86}Y-CHX-A″-DTPA-bevacizumab conjugate was successfully prepared, with radiochemical yields ranging from 60 to 75% and specific activities exceeding 1.5 GBq/mg. The chelate to protein ratio determined by arsenazo assay was 1.9. The absolute binding determined by RIA ranged from 58–66 % and the non-specific binding was less than 6 %.

In vivo evaluations

Biodistribution studies and pharmacokinetic analysis—In mice bearing VEGF-A secreting SKOV3 and VEGF-A negative MSTO-211H tumor xenografts, approximately 50% decrease in the blood pool activity was observed over a 4 d time period (10.57 ± 1.62 % ID/g at 0.5 d to 5.84 ± 0.61 % ID/g at 4 d) (Fig 1). Similarly, approximately 50 % decrease was observed in liver uptake over a 4 d time period (13.87 ± 0.80 % ID/g at 0.5 d to 7.87 ± 0.60 % ID/g at 4 d) (Fig 1). An opposite trend was observed in VEGF-A secreting SKOV3 tumor uptake, with the % ID/g of 11.73 ± 1.80 observed at 0.5 d increasing to 15.12 ± 0.74 at 4 d after injection (Fig. 1). In comparison, the uptake in VEGF-A negative MSTO-211H tumor did not alter significantly at 0.5 d (5.40 ± 0.81 % ID/g) and 4 d (5.89 ± 0.16 % ID/g). The SKOV3 tumor-to-blood ratio increased more than 2-fold from 1.1 at 0.5 d to 2.6 at 4 d after injection.

The ^{86}Y-CHX-A″-DTPA-bevacizumab uptake in VEGF-A secreting SKOV3 and LS-174T tumors was VEGF-A-mediated as demonstrated by the blocking experiments performed by co-injecting 0.05 mg bevacizumab (Fig 2). In mice bearing VEGF-A secreting SKOV3 and VEGF-A negative MSTO-211H (Fig. 2A), and VEGF-A secreting LS-174T (Fig. 2B) tumors, the tumor % ID/g at 3 d was 17.40 ± 1.70, 6.28 ± 0.67 and 13.55 ± 1.49, respectively. The corresponding tumor % ID/g in mice co-injected with 0.05 mg bevacizumab was 8.94 ± 1.95, 7.44 ± 1.0 and 5.77 ± 1.3. Statistically significant reduction in uptake was observed in VEGF-A secreting SKOV3 and LS-174T tumors, while no difference in uptake was observed in VEGF-A negative MSTO-211H tumor xenografts in these blocking studies, demonstrating specificity of the RIC (Fig. 2).

To study the overall accumulation of the RIC in the tumors, AUC and AUMC analyses were performed. VEGF-A secreting SKOV3 tumors had the highest AUC (47.7 ± 3.1 %ID.d.g^{-1}) and AUMC (126.1 ± 9.9 %ID.d^2.g^{-1}), followed by LS-174T tumors as shown in Table 1. The tracer accumulation in the VEGF-A secreting SKOV3 and LS-174T tumors was

significantly higher ($p < 0.05$) than VEGF-A negative MSTO-211H tumors (Table 1). However, the tumor MRT was identical for all three tumors (2.6–2.7 d).

PET imaging studies—The linearity of the PET-assessed concentration *vs*. the radioactivity concentration measured in a Capintec CRC-127R dose calibrator was $r^2 = 0.99$ in the radioactivity range of 0.03–4.00 MBq/mL of ^{86}Y solution from cylindrical phantom studies.

Small animal PET imaging studies were performed in female athymic mice bearing VEGF-A secreting SKOV-3 on one leg and VEGF-A negative MSTO-211H on another (Fig. 3A) injected with 1.8–2.0 MBq of ^{86}Y-CHX-A″-DTPA-bevacizumab or ^{86}Y-CHX-A″-DTPA-bevacizumab co-injected with 0.05 mg bevacizumab (Fig. 3B). The SKOV3 tumors were clearly visualized in maximum intensity projections (top panel) and transverse slices (bottom panel) of mice imaged from 1 to 3 d after injection of the RIC, whereas VEGF-A negative MSTO-211H tumor could not be visualized due to lack of significant accumulation of the radiotracer (Fig. 3A). The SKOV3 tumor-to-background ratios improved over the period mostly due to the clearance of in the RIC from the blood while the tumor uptake increased (Fig. 4A). In contrast, when 0.05 mg of bevacizumab was co-injected with the RIC, the tumors were poorly visualized due to target-specific blockage, demonstrating the VEGF-A-specificity of ^{86}Y-CHX-A″-DTPA-bevacizumab (Fig. 3B and 4A). As shown in Table 1, the AUCs derived from the quantitated SKOV3 and LS-174T tumor uptake values of mice injected with ^{86}Y-CHX-A″-DTPA-bevacizumab and mice injected with ^{86}Y-CHX-A″-DTPA-bevacizumab and 0.05 mg unlabeled bevacizumab were significantly different while the MSTO-211H PET derived tumor AUC uptake was not (Table 1). For mice bearing SKOV3 tumors, the PET assessed tumor $AUC_{[0\rightarrow t]}$ of mice injected with ^{86}Y-CHX-A″-DTPA-bevacizumab was 2.2 times greater than that of mice co-injected with 0.05 mg bevacizumab (Table 1). The *in vivo* tumor uptake quantified by PET at all time points closely correlated ($r^2 = 0.87$, $p = 0.64$, n=18) to values determined by *ex vivo* biodistribution studies (Fig. 4B).

Discussion

The existence of tumor-derived factors responsible for promoting new blood vessel growth was postulated almost more than half a century ago [20, 21]. In 1971, it was hypothesized that inhibition of angiogenesis could be an effective approach for the treatment of cancer [22]. Since then, extensive research has been carried out to identify and target several regulators of angiogenesis such as VEGF [2]. In February 2004, the US FDA approved bevacizumab, a humanized anti-VEGF A monoclonal antibody, for the treatment of metastatic colorectal cancer in combination with 5-fluorouracil (FU)-based chemotherapy regimens [23]. Since then, the US FDA has approved several anti-angiogenic agents such as pegaptanib, sorafenib and ranibizumab. These developments have validated the notion of angiogenesisis as an important target for cancer and other diseases. However, further progress is warranted on a variety of important issues; including the selection of patients that are most likely to respond to a particular anti-angiogenic treatment. Towards this end, molecular imaging, with PET/SPECT and MRI, has been explored as a possible way to select and screen patients for anti-angiogenic therapy. In this study, a potential PET agent, ^{86}Y labeled bevacizumab for selecting and screening patients for bevacizumab related therapy and as a surrogate marker for ^{90}Y-RIT is presented. Initially, at the time of this study, the approach of using radiolabeled bevacizumab for imaging was viewed with a certain amount of skepticism since VEGF is diffusible and breaks down very quickly. Tumor to background ratios were therefore envisaged to be poor. In the past two years however, two studies reported the use of radiolabeled bevacizumab for imaging tumor angiogenesis in preclinical models [10, 11]. After further investigation, it was found that the accumulation of the radiolabeled

bevacizumab in the tumor was due to its interaction with the VEGF-A 165 and 189 isoforms associated with the tumor cell surface and/or the extracellular matrix [24]. In a clinical study, the tumor accumulation of ^{111}In-bevacizumab and VEGF-A expression in patients with colorectal liver metastases was investigated[12]. Enhanced uptake of ^{111}In-bevacizumab in liver metastases was observed in 9 out of 12 patients, although no correlation between the level of antibody accumulation and expression of VEGF-A was found [12].

The straightforward preparation of high specific activity ^{86}Y-CHX-A″-DTPA-bevacizumab reported in this study along with the direct incorporation of ^{86}Y by the CHX-A″-DTPA-bevacizumab at room temperature in less than an hour offers an advantage over previously reported preparation of ^{89}Zr labeled bevacizumab. Although ^{111}In labeled bevacizumab has already been explored in the clinic, SPECT as an imaging modality has intrinsic limitations with respect to quantification, primarily because of insufficient correction of scatter and partial absorption of gamma-photons in the tissue. Due to better and more accurate scatter and attenuation corrections associated with PET, ^{86}Y labeled bevacizumab was developed for imaging VEGF-A tumor angiogenesis and as a surrogate marker for ^{90}Y based RIT. The ^{111}In and ^{89}Zr labeled probes have been proposed as surrogate imaging markers for ^{90}Y therapy, howeverdeviations were observed due to subtle differences in the metal–chelate complexes and metabolism [25, 26], highlighting the need for the development of isotopically matched ^{86}Y labeled probes for ^{90}Y.

However, ^{86}Y posses its own set of challenges, in particular, its high positron energy (E_{max} = 3.1 MeV) and γ-emission of 1.08 MeV (83% abundance) which can significantly affect the image quality and recovery coefficients due to spurious coincidences [16]. When appropriate corrections are performed, the image quality is greatly improved and is quantifiable as shown in this study as well as by others [27–29]. In this study, normalization experiments were performed with a cylinder phantom filled with a solution of ^{86}Y during each imaging session to apply appropriate corrections. After partial volume, scatter and background corrections, the *in vivo* tumor uptake quantified by PET correlated (r^2= 0.87, p= 0.64, n=18) with the values determined by *ex vivo* biodistribution studies at 1, 2 and 3 d after injection.

PET imaging with ^{86}Y-CHX-A″-DTPA-bevacizumab may have a useful role in patient selection for bevacizumab related therapy since it would indicate accessibility of the antibody to VEGF-A target sites. However, ^{86}Y-CHX-A″-DTPA-bevacizumab imaging by itself may not predict the response to therapy as it is only indicative of how much bevacizumab reaches the tumor and not the overall tumor microenvironment and the biomolecular characteristics. The primary use of ^{86}Y-CHX-A″-DTPA-bevacizumab will be for the selection of patients for ^{90}Y-CHX-A″-DTPA-bevacizumab RIT, monitoring of those patients during therapy as well as to provide information for dosimetry calculations as previously suggested [17, 25]. To achieve the long-term goal of clinical translation of ^{86}Y-CHX-A″-DTPA-bevacizumab, PET/CT and MRI studies are currently being performed with mice bearing orthotopic and disseminated ascites forming colorectal and ovarian tumors.

In conclusion, the utility of ^{86}Y-CHX-A″-DTPA-bevaciuzmab for non-invasive PET imaging of VEGF-A secreting tumors in preclinical models has been demonstrated. ^{86}Y-CHX-A″-DTPA-bevacizumab may be useful for the assessment of bevacizumab uptake and localization, which may be important for risk stratification, patient screening and appropriate dosage selection. Ultimately, ^{86}Y-CHX-A″-DTPA-bevacizumab would serve as a surrogate PET marker for dosimetry and selection of subjects for ^{90}Y CHX-A″-DTPA-bevacizumab RIT of VEGF-A secreting cancers.

Acknowledgments

This research was supported by the Intramural Research Program of the National Institute of Health, National Cancer Institute, Center for Cancer Research and the United States Department of Health and Human Services.

References

1. Hanahan D, Weinberg RA. The hallmarks of cancer. Cell. 2000; 100:57–70. [PubMed: 10647931]
2. Ferrara N, Kerbel RS. Angiogenesis as a therapeutic target. Nature. 2005; 438:967–74. [PubMed: 16355214]
3. Ferrara N, Gerber HP, LeCouter J. The biology of VEGF and its receptors. Nat Med. 2003; 9:669–76. [PubMed: 12778165]
4. Folkman J. Role of angiogenesis in tumor growth and metastasis. Semin Oncol. 2002; 29:15–8. [PubMed: 12516034]
5. Ferrara N, Hillan KJ, Gerber HP, Novotny W. Discovery and development of bevacizumab, an anti-VEGF antibody for treating cancer. Nat Rev Drug Discov. 2004; 3:391–400. [PubMed: 15136787]
6. Grothey A, Galanis E. Targeting angiogenesis: progress with anti-VEGF treatment with large molecules. Nat Rev Clin Oncol. 2009; 6:507–18. [PubMed: 19636328]
7. O'Connor JP, Carano RA, Clamp AR, Ross J, Ho CC, Jackson A, Parker GJ, Rose CJ, Peale FV, Friesenhahn M, Mitchell CL, Watson Y, et al. Quantifying antivascular effects of monoclonal antibodies to vascular endothelial growth factor: insights from imaging. Clin Cancer Res. 2009; 15:6674–82. [PubMed: 19861458]
8. Zwick S, Strecker R, Kiselev V, Gall P, Huppert J, Palmowski M, Lederle W, Woenne EC, Hengerer A, Taupitz M, Semmler W, Kiessling F. Assessment of vascular remodeling under antiangiogenic therapy using DCE-MRI and vessel size imaging. J Magn Reson Imaging. 2009; 29:1125–33. [PubMed: 19388117]
9. de Groot JF, Fuller G, Kumar AJ, Piao Y, Eterovic K, Ji Y, Conrad CA. Tumor invasion after treatment of glioblastoma with bevacizumab: radiographic and pathologic correlation in humans and mice. Neuro Oncol. 12:233–42. [PubMed: 20167811]
10. Nagengast WB, de Vries EG, Hospers GA, Mulder NH, de Jong JR, Hollema H, Brouwers AH, van Dongen GA, Perk LR, Lub-de Hooge MN. In vivo VEGF imaging with radiolabeled bevacizumab in a human ovarian tumor xenograft. J Nucl Med. 2007; 48:1313–9. [PubMed: 17631557]
11. Stollman TH, Scheer MG, Leenders WP, Verrijp KC, Soede AC, Oyen WJ, Ruers TJ, Boerman OC. Specific imaging of VEGF-A expression with radiolabeled anti-VEGF monoclonal antibody. Int J Cancer. 2008
12. Scheer MG, Stollman TH, Boerman OC, Verrijp K, Sweep FC, Leenders WP, Ruers TJ, Oyen WJ. Imaging liver metastases of colorectal cancer patients with radiolabelled bevacizumab: Lack of correlation with VEGF-A expression. Eur J Cancer. 2008; 44:1835–40. [PubMed: 18632262]
13. Garmestani K, Milenic DE, Plascjak PS, Brechbiel MW. A new and convenient method for purification of 86Y using a Sr(II) selective resin and comparison of biodistribution of 86Y and 111In labeled Herceptin. Nucl Med Biol. 2002; 29:599–606. [PubMed: 12088731]
14. Nayak TK, Garmestani K, Baidoo K, Milenic D, Brechbiel M. Quantitative PET imaging of cancer using the human anti-HER1 monoclonal antibody, panitumumab labeled with Y86. J NUCL MED MEETING ABSTRACTS. 2009; 50:1911–11.
15. Nayak TK, Regino CA, Wong KJ, Milenic DE, Garmestani K, Baidoo KE, Szajek LP, Brechbiel MW. PET imaging of HER1-expressing xenografts in mice with (86)Y-CHX-A″-DTPA-cetuximab. Eur J Nucl Med Mol Imaging. In press. 10.1007/s00259–009–1370-z
16. Nayak TK, Brechbiel MW. Radioimmunoimaging with Longer-Lived Positron-Emitting Radionuclides: Potentials and Challenges. Bioconjug Chem. 2009; 20:825–41. [PubMed: 19125647]
17. Palm S, Enmon RM Jr, Matei C, Kolbert KS, Xu S, Zanzonico PB, Finn RL, Koutcher JA, Larson SM, Sgouros G. Pharmacokinetics and Biodistribution of (86)Y-Trastuzumab for (90)Y dosimetry

in an ovarian carcinoma model: correlative MicroPET and MRI. J Nucl Med. 2003; 44:1148–55. [PubMed: 12843231]

18. Pippin CG, Parker TA, McMurry TJ, Brechbiel MW. Spectrophotometric method for the determination of a bifunctional DTPA ligand in DTPA-monoclonal antibody conjugates. Bioconjug Chem. 1992; 3:342–5. [PubMed: 1390990]
19. Li Q, Yano S, Ogino H, Wang W, Uehara H, Nishioka Y, Sone S. The therapeutic efficacy of anti vascular endothelial growth factor antibody, bevacizumab, and pemetrexed against orthotopically implanted human pleural mesothelioma cells in severe combined immunodeficient mice. Clin Cancer Res. 2007; 13:5918–25. [PubMed: 17908988]
20. Ide AG, Baker NH, Warren SL. Vascularization of the Brown Pearce rabbit epithelioma transplant as seen in the transparent ear chamber. Am J Roentgenol. 1939; 42:891–9.
21. Algire GH, Legallais FY. Growth and vascularization of transplanted mouse melanomas. Ann N Y Acad Sci. 1948; 4:159–70. [PubMed: 18862169]
22. Folkman J. Tumor angiogenesis: therapeutic implications. N Engl J Med. 1971; 285:1182–6. [PubMed: 4938153]
23. Hurwitz H, Fehrenbacher L, Novotny W, Cartwright T, Hainsworth J, Heim W, Berlin J, Baron A, Griffing S, Holmgren E, Ferrara N, Fyfe G, et al. Bevacizumab plus irinotecan, fluorouracil, and leucovorin for metastatic colorectal cancer. N Engl J Med. 2004; 350:2335–42. [PubMed: 15175435]
24. Stollman TH, Scheer MG, Franssen GM, Verrijp KN, Oyen WJ, Ruers TJ, Leenders WP, Boerman OC. Tumor accumulation of radiolabeled bevacizumab due to targeting of cell- and matrix-associated VEGF-A isoforms. Cancer Biother Radiopharm. 2009; 24:195–200. [PubMed: 19409041]
25. Helisch A, Forster GJ, Reber H, Buchholz HG, Arnold R, Goke B, Weber MM, Wiedenmann B, Pauwels S, Haus U, Bouterfa H, Bartenstein P. Pre-therapeutic dosimetry and biodistribution of 86Y-DOTA-Phe1-Tyr3-octreotide versus 111In-pentetreotide in patients with advanced neuroendocrine tumours. Eur J Nucl Med Mol Imaging. 2004; 31:1386–92. [PubMed: 15175836]
26. Perk LR, Visser OJ, Stigter-van Walsum M, Vosjan MJ, Visser GW, Zijlstra JM, Huijgens PC, van Dongen GA. Preparation and evaluation of (89)Zr-Zevalin for monitoring of (90)Y-Zevalin biodistribution with positron emission tomography. Eur J Nucl Med Mol Imaging. 2006; 33:1337–45. [PubMed: 16832633]
27. Liu X, Laforest R. Quantitative small animal PET imaging with nonconventional nuclides. Nucl Med Biol. 2009; 36:551–9. [PubMed: 19520296]
28. Herzog H, Tellmann L, Scholten B, Coenen HH, Qaim SM. PET imaging problems with the non-standard positron emitters Yttrium-86 and Iodine-124. Q J Nucl Med Mol Imaging. 2008; 52:159–65. [PubMed: 18043538]
29. Buchholz HG, Herzog H, Forster GJ, Reber H, Nickel O, Rosch F, Bartenstein P. PET imaging with yttrium-86: comparison of phantom measurements acquired with different PET scanners before and after applying background subtraction. Eur J Nucl Med Mol Imaging. 2003; 30:716–20. [PubMed: 12605273]

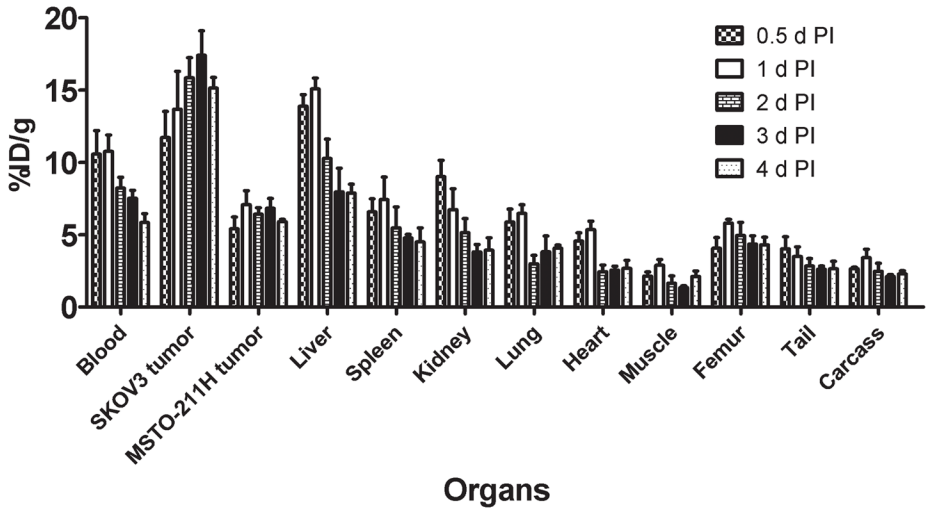

Figure 1.

Uptake values of ^{86}Y-CHX-A″-DTPA-bevacizumab in selected organs of female athymic (NCr) *nu/nu* mice bearing VEGF-A positive human ovarian carcinoma SKOV3 xenografts and VEGF-A negative human biphasic mesothelioma MSTO-211 xenografts. Biodistribution data were obtained at 0.5, 1, 2, 3 and 4 d after injection. All uptake values are expressed as %ID/g. Data represent the mean value ± SEM from at least four determinations.

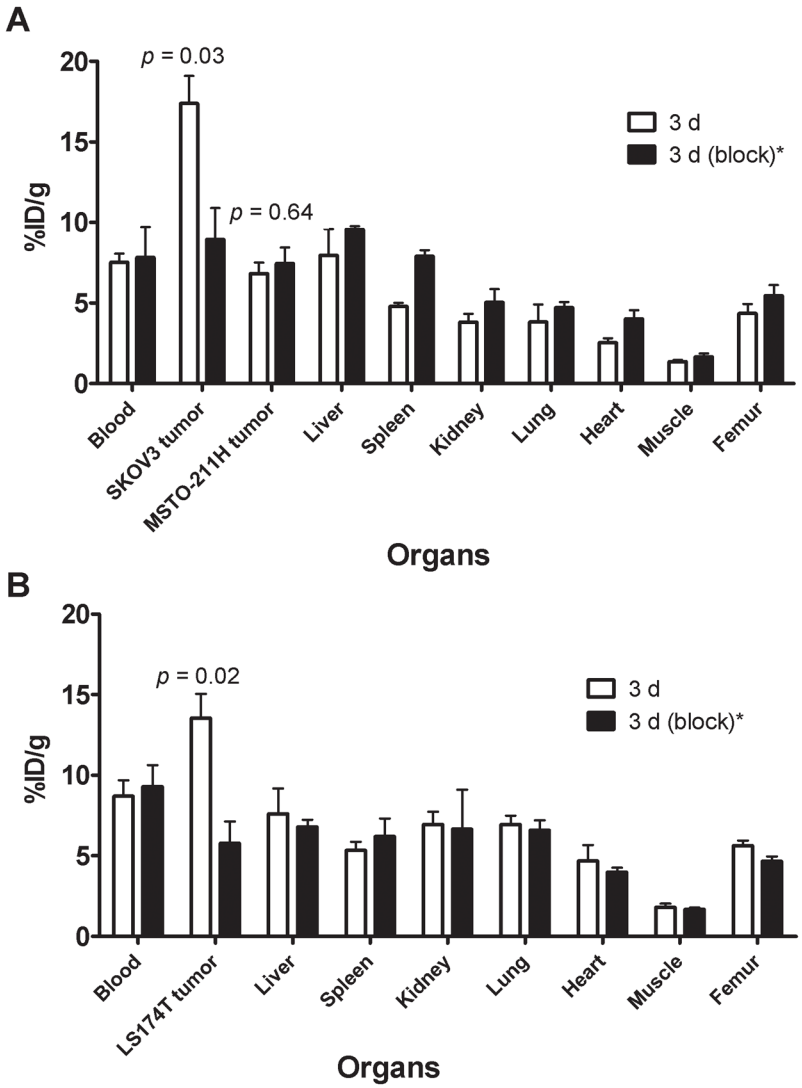

Figure 2.

Receptor-meditated uptake of ^{86}Y-CHX-A″-DTPA-bevacizumab in selected organs of female athymic (NCr) *nu/nu* mice bearing bearing VEGF-A positive human ovarian carcinoma SKOV3 xenografts and VEGF-A negative human biphasic mesothelioma MSTO-211 xenografts **(A)** and VEGF-A positive human colorectal carcinoma LS-174T xenografts **(B)**. Biodistribution data were obtained at 3 d after injection. All uptake values are expressed as %ID/g. Data represent the mean value ± SEM from at least four determinations.

*Receptor blocking studies were performed by co-injecting 0.05 mg bevacizumab with the RIC.

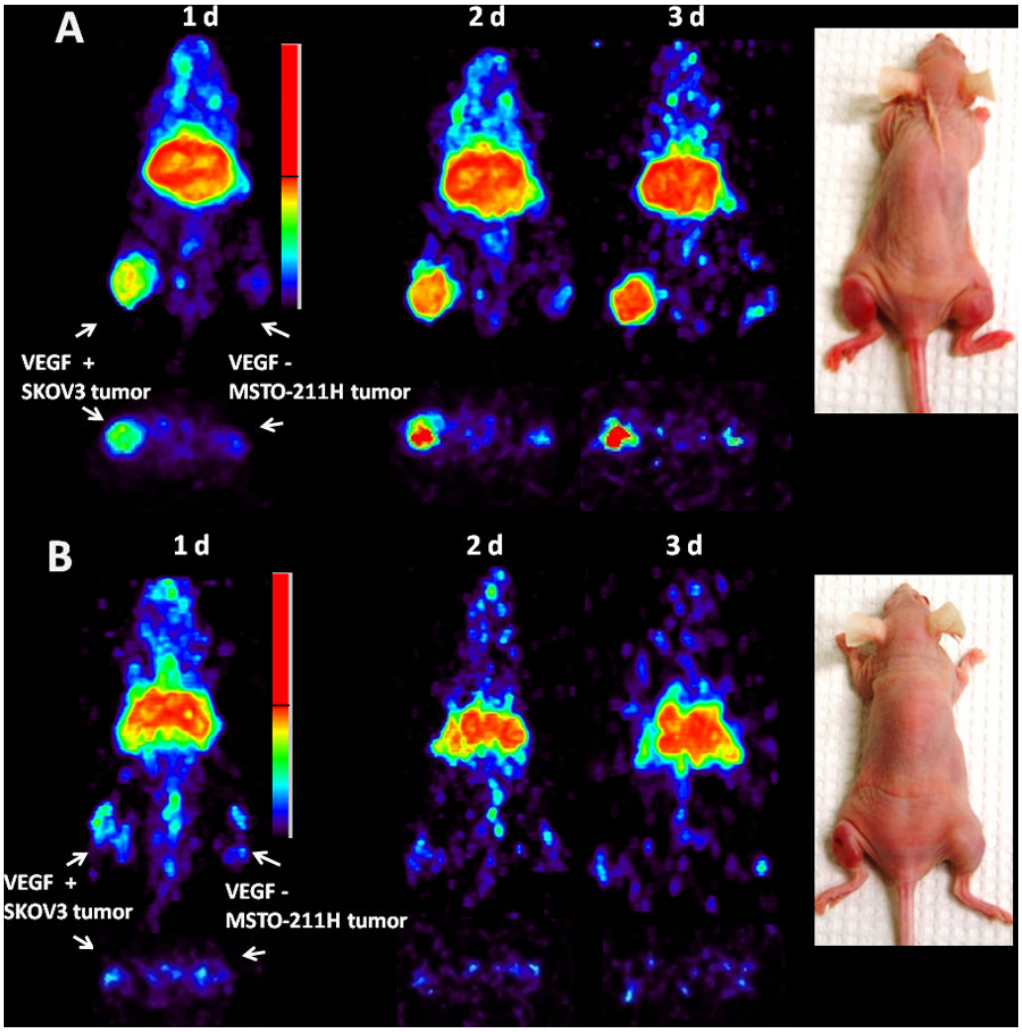

Figure 3.

(A) Representative reconstructed and processed maximum intensity projections (top panel) and transverse slices (bottom panel) of female athymic (NCr) *nu/nu* mouse bearing VEGF-A positive human ovarian carcinoma SKOV3 xenograft on one leg and VEGF-A negative human biphasic mesothelioma MSTO-211H on another leg injected i.v. via tail vein with 1.8–2.0 MBq of ^{86}Y-CHX-A″-DTPA-bevacizumab. (B) Female athymic (NCr) *nu/nu* mouse bearing VEGF-A positive human ovarian carcinoma SKOV3 xenograft on one leg and VEGF-A negative human biphasic mesothelioma MSTO-211H on another leg injected i.v. via tail vein with 1.8–2.0 MBq of ^{86}Y-CHX-A″-DTPA-bevacizumab and 0.05 mg bevacizumab for blocking VEGF-A. The tumors are shown with a white arrow in the images.

*Receptor blocking studies were performed by co-injecting 0.05 mg bevacizumab with the RIC.

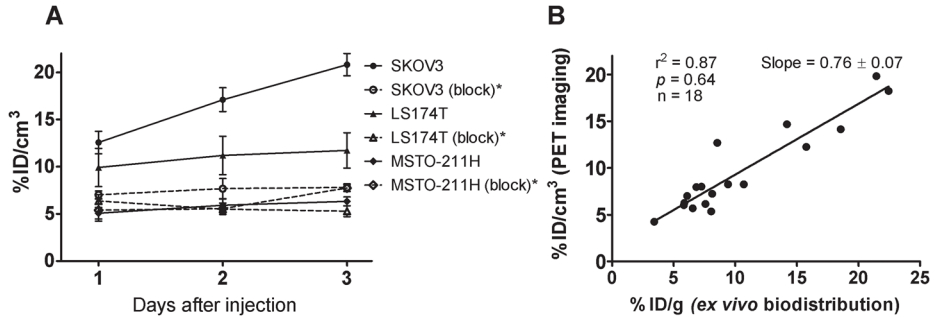

Figure 4.

(A) Time-activity curve and uptake values of ^{86}Y-CHX-A″-DTPA-bevacizumab in female athymic (NCr) *nu*/*nu* mice bearing VEGF-A positive SKOV3, LS-174T and VEGF-A negative MSTO-211H tumor xenografts. **(B)** Correlation between organ uptake values assessed through *ex vivo* biodistribution studies and quantitative small animal PET imaging. All uptake values derived from PET studies are expressed as % ID/cm^3. Data represent the mean value ± SEM from three determinations.

*Receptor blocking studies performed by co-injecting 0.05 mg bevacizumab with the radiotracer.

Table 1

Pharmacokinetic characteristics of ^{86}Y-CHX-A″-DTPA-bevacizumab injected i.v. via tail vein of female athymic (NCr) *nu*/*nu* mice bearing VEGF-A positive SKOV3, LS-174T and VEGF-A negative MSTO-211H tumor xenografts. Data represent the mean values from three to four determinations.

Pharmacokinetic characteristics	SKOV3 (Ovarian)	LS174T (Colorectal)	MSTO-211H (Mesothelioma)
Tumor $AUC_{[0\rightarrow4]}$ (%ID.d.g^{-1})	47.7 ± 3.1	36.6 ± 3.2	19.8 ± 1.6
Tumor PET $AUC_{[0\rightarrow3]}$ (%ID.d.cc^{-1})	33.8 ± 1.8	22.5 ± 3.5	11.6 ± 1.3
Tumor PET $AUC_{[0\rightarrow3]}$ (%ID.d.cc^{-1})*	15.1 ± 1.2	11.3 ± 0.9	12.1 ± 1.2
Tumor $AUMC_{[0\rightarrow4]}$ (%ID.d^2.g^{-1})	126.1 ± 9.9	98.9 ± 8.6	52.1± 4.8
Tumor MRT (d)	2.7	2.6	2.6

*Receptor blocking studies performed by co-injecting 0.05 mg bevacizumab with the radiotracer